Electronic Supplementary Material (ESI) for Nanoscale.

Supporting information for: Structural Evolution of Iron Forming Iron Oxide in a Deep Eutectic-Solvothermal Reaction

Oliver S. Hammond,[1,] Ria S. Atri,[1] Daniel T. Bowron,[2] Liliana de Campo,[3] Sofia Diaz-Moreno,[4] Luke Keenan,[4] James Doutch,[5] Salvador Eslava,[5] and Karen J. Edler[1,*]*

[1]Department of Chemistry and Centre for Doctoral Training in Sustainable Chemical Technologies, University of Bath, Claverton Down, Bath BA2 7AY, UK.

[2]ISIS Neutron and Muon Source, Science and Technology Facilities Council, Rutherford Appleton Laboratory, Didcot OX11 0QX, UK.

[3]Australian Centre for Neutron Scattering, ANSTO, Lucas Heights, New South Wales 2234, Australia

[4]Diamond Light Source, Science and Technology Facilities Council, Rutherford Appleton Laboratory, Didcot OX11 0QX, UK.

[5]Department of Chemical Engineering, University of Bath, Claverton Down, Bath BA2 7AY, UK.

* oliver.hammond@mmk.su.se

* k.edler@bath.ac.uk

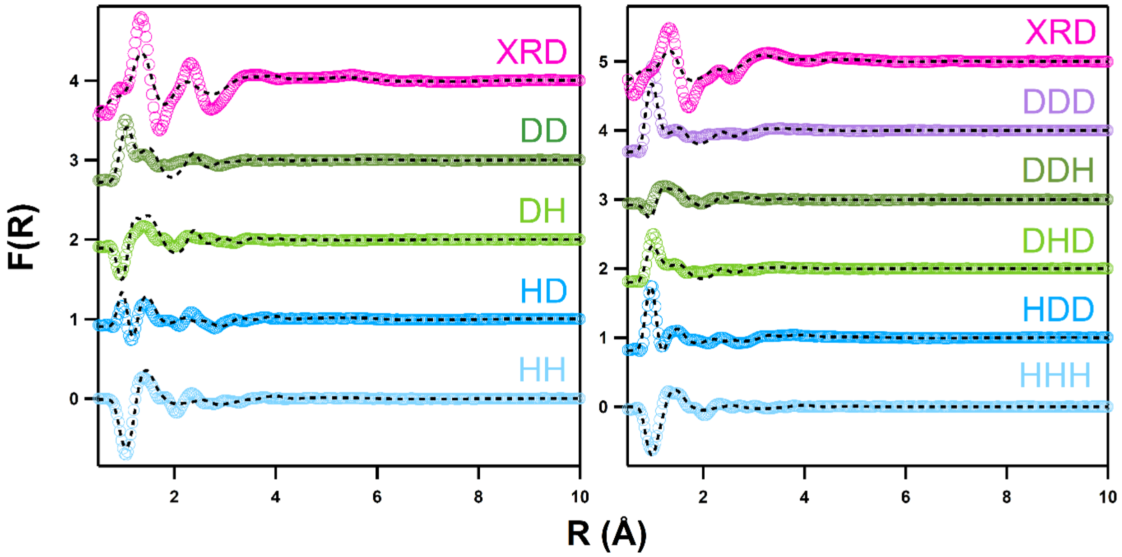

Figure S1. Neutron and X-Ray diffraction data (coloured markers) and fits to the data (black dashed lines) shown Fourier-transformed into R-space, for the pure choline chloride:urea DES (left) and the hydrated choline chloride:urea:10 H_2O DES (right), containing 0.25 mol kg^{-1} $Fe(NO_3)_3.9H_2O$.

Table S1. Calculated partial (site-site) coordination numbers for the pure and hydrated choline chloride:urea DES containing 0.25 mol kg^{-1} of $Fe(NO_3)_3.9H_2O$. As with the molecular radial distribution function presented in Table 2 of the main text, partial radial distribution functions are presented as ensemble averages, with the associated standard deviation, of 10000 iterations of the model as it evolves within the confines of the empirical potential. Coordination numbers are calculated by integrating each pRDF to their first minima; R_{max} describes this maximum radius of integration.

‘A'	‘B'	R_{max} (0w) (Å)	R_{max} (10w) (Å)	N_{coord} (1w) Pure solvent	N_{coord} (0w) With [Fe]	N_{coord} (10w) Pure solvent	N_{coord} (10w) With [Fe]
Cl	C_U	5.0	5.2	3.25 ± 1.49	3.11 ± 1.43	1.79 ± 1.24	1.34 ± 1.01
Cl	N_U	3.9	4.1	3.10 ± 1.67	2.96 ± 1.59	1.71 ± 1.39	1.07 ± 0.99
Cl	H_{U1}	3.0	3.0	1.52 ± 1.36	1.31 ± 1.13	0.76 ± 1.00	0.43 ± 0.64
Cl	H_{U2}	3.0	3.0	1.02 ± 0.93	1.20 ± 1.02	0.44 ± 0.65	0.36 ± 0.58
H_{OH}	Cl	3.2	3.2	0.55 ± 0.51	0.32 ± 0.49	0.35 ± 0.48	0.12 ± 0.33
M_T	Cl	4.0	4.0	0.59 ± 0.62	0.58 ± 0.67	0.30 ± 0.49	0.23 ± 0.45
H_{CN}	Cl	4.0	4.0	0.59 ± 0.61	0.51 ± 0.62	0.33 ± 0.51	0.21 ± 0.44
H_{CO}	Cl	4.0	4.0	0.59 ± 0.62	0.45 ± 0.60	0.32 ± 0.51	0.17 ± 0.41
H_{CN}	O_U	3.5	3.5	0.48 ± 0.62	0.65 ± 0.68	0.22 ± 0.45	0.34 ± 0.53
M_T	O_U	3.4	3.5	0.52 ± 0.65	0.50 ± 0.63	0.25 ± 0.47	0.35 ± 0.55
H_{CO}	O_U	3.6	3.6	0.54 ± 0.67	0.66 ± 0.70	0.27 ± 0.49	0.25 ± 0.46
H_{OH}	O_U	2.5	2.5	0.19 ± 0.40	0.30 ± 0.47	0.10 ± 0.30	0.14 ± 0.35
H_{OH}	N_U	4.3	4.3	2.49 ± 1.60	3.14 ± 1.65	1.21 ± 1.19	1.31 ± 1.23
N	N	6.8	7.3	2.61 ± 1.28	2.41 ± 1.05	1.88 ± 1.25	1.46 ± 1.05
N	C_{2N}	7.5	7.7	4.98 ± 1.58	4.86 ± 1.28	3.41 ± 1.43	2.84 ± 1.21
N	C_{OH}	6.2	6.4	2.88 ± 1.24	2.68 ± 1.05	2.09 ± 1.01	1.85 ± 0.81
N	O_H	5.2	5.4	2.08 ± 0.98	2.13 ± 0.92	1.62 ± 0.77	1.59 ± 0.68
N	H_{OH}	5.5	5.8	2.36 ± 1.10	2.45 ± 1.04	1.84 ± 0.90	1.78 ± 0.75
O_U	N_U	3.5	3.6	3.31 ± 1.05	2.98 ± 0.92	2.78 ± 0.89	2.63 ± 0.79

O_U	**H_{U1}**	2.6	2.6	0.46 ± 0.73	0.36 ± 0.58	0.25 ± 0.55	0.21 ± 0.45
O_U	**H_{U2}**	2.6	2.6	1.73 ± 0.87	2.06 ± 0.79	1.51 ± 0.77	1.87 ± 0.67
N_U	**H_{U1}**	4.6	4.6	4.87 ± 2.01	4.75 ± 1.96	3.49 ± 1.60	3.30 ± 1.52
N_U	**H_{U2}**	4.6	4.6	4.97 ± 1.78	5.01 ± 1.75	3.57 ± 1.45	3.49 ± 1.39
Cl	**Cl**	6.0	6.0	1.23 ± 0.91	1.93 ± 1.50	0.58 ± 0.69	1.22 ± 1.15
N	**O_1**	5.8	5.4	2.09 ± 1.41	2.18 ± 1.60	10.21 ± 2.42	9.94 ± 2.23
H_{OH}	**O_1**	2.3	2.3	0.07 ± 0.26	0.12 ± 0.33	0.35 ± 0.48	0.54 ± 0.51
H_{CN}	**O_1**	3.5	3.6	0.28 ± 0.52	0.25 ± 0.50	1.61 ± 1.05	1.88 ± 1.07
H_{CO}	**O_1**	3.6	3.6	0.32 ± 0.56	0.36 ± 0.59	1.75 ± 1.12	2.24 ± 1.10
Cl	**O_1**	4.3	4.2	1.09 ± 1.03	1.13 ± 1.12	5.12 ± 1.66	6.15 ± 1.69
O_1	**O_1**	4.2	3.4	0.99 ± 1.02	0.85 ± 0.81	2.70 ± 1.16	2.89 ± 1.19

Values are compared with data in the pure solvent for containing 10*w* (41 wt%) for the hydrated system and 1*w* (6.5 wt%) for the 'pure' system, as published previously.[27] This is because the pure 1*w* solvent is closer in hydration to the pure solvent with 0.25 mol kg^{-1} of iron nitrate nonahydrate, which contains 3.7 wt% water, whereas the analysis of the pure iron-free DES was assumed to be anhydrous.[35]

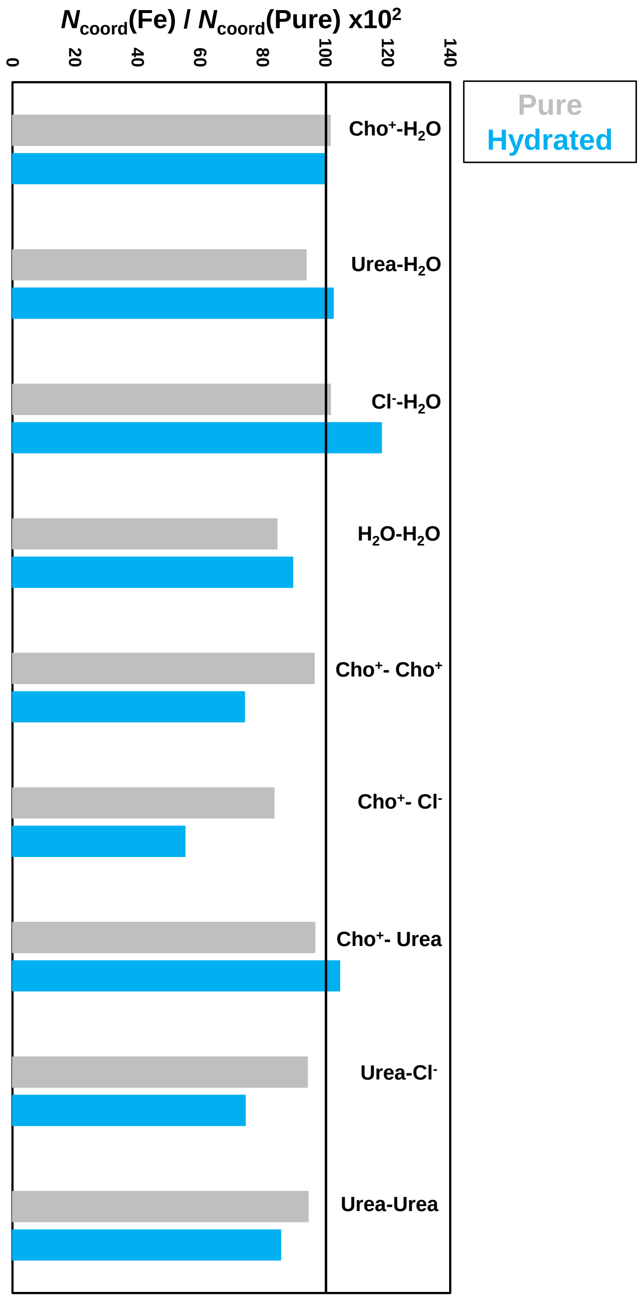

Figure S2. Percentage change in intermolecular radial distribution functions for the pure and hydrated DES when iron nitrate salt is added at 0.25 mol kg^{-1}, calculated from the values shown in Table S1. Values are relative to the coordination number seen in the pure solvent without salt, which is choline chloride:urea 10*w* for the hydrated system, and 1*w* for the 'pure' system, which contains 3.7 wt% water from the iron nitrate water of crystallisation. A tie line is drawn at the 100% level.

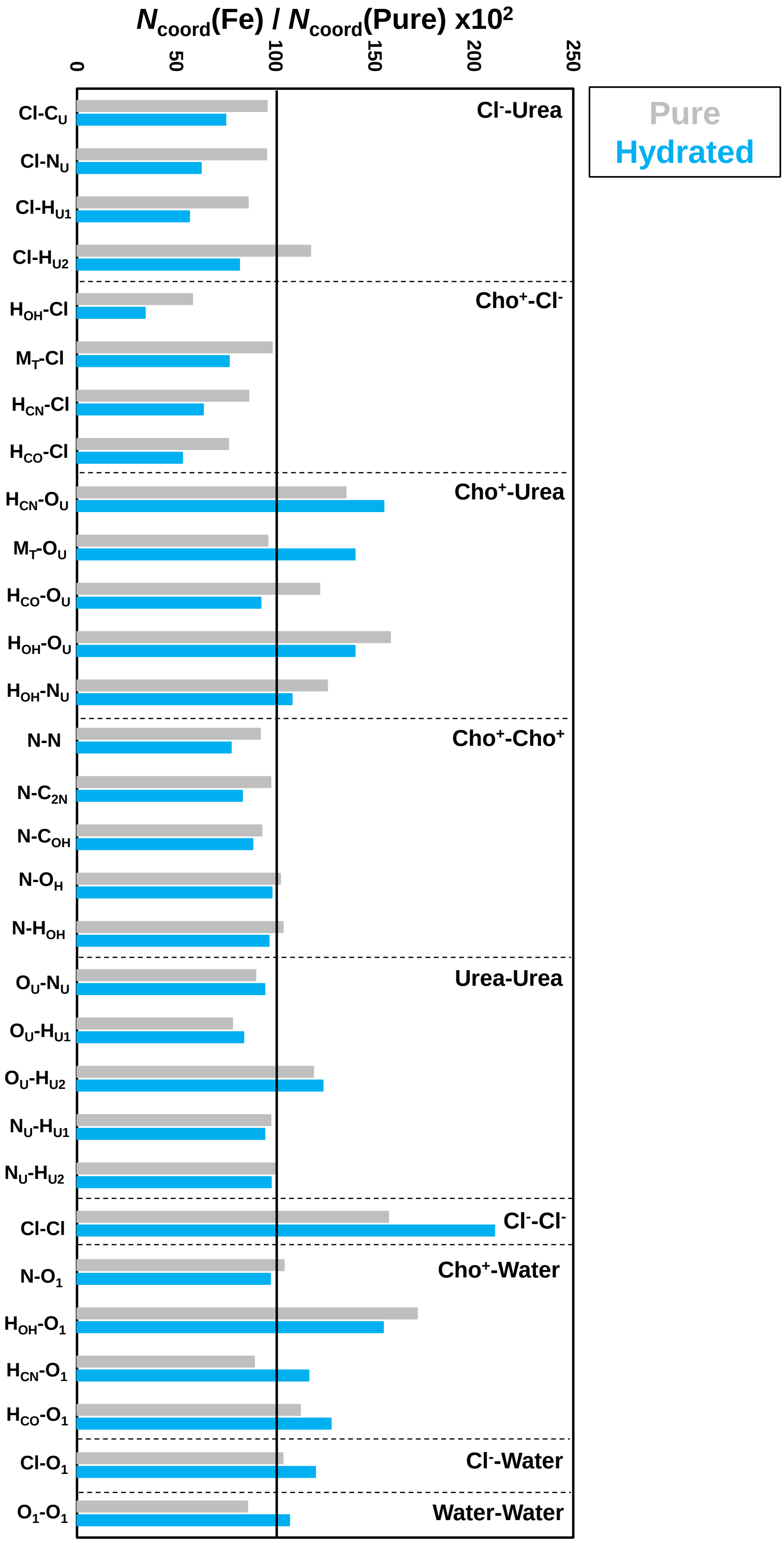

Figure S3. Percentage change in partial radial distribution functions for the pure and hydrated DES when iron nitrate salt is added at 0.25 mol kg^{-1}, calculated from the values shown in Table S1. Values are relative to the coordination number seen in the pure solvent without salt, which is choline chloride:urea 10*w* for the hydrated system, and 1*w* for the 'pure' system, which contains 3.7 wt% water from the iron nitrate water of crystallisation. A tie line is drawn at the 100% level.

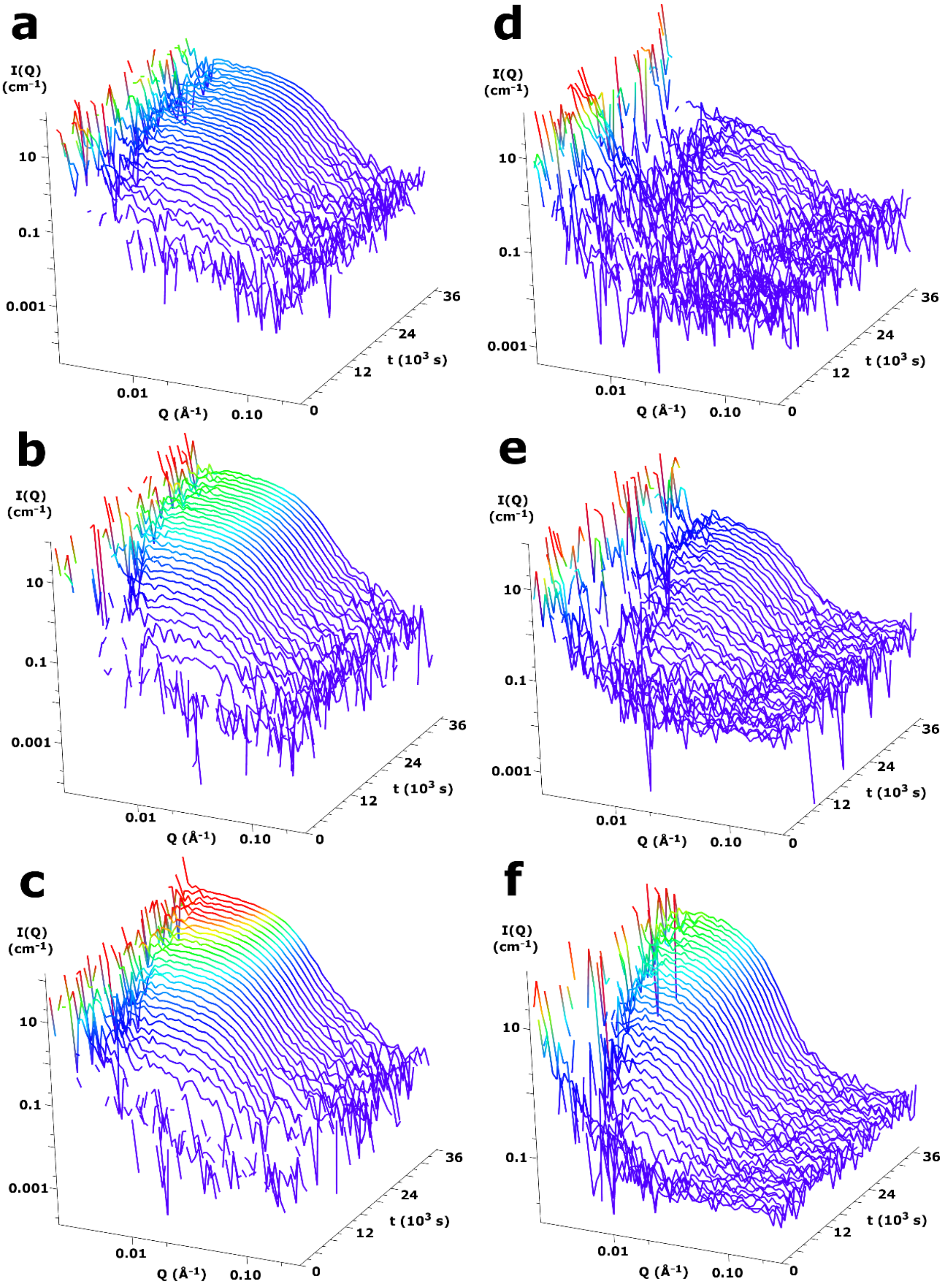

Figure S4. Time-resolved SANS data taken for the pure DES as a function of initial $Fe(NO_3)_3.9H_2O$ mole fraction; (a-c) choline chloride:urea isotopic composition of H:D; (d-f) choline chloride:urea isotopic composition of D:D; (a,d) 0.15 mol kg^{-1}, (b,e) 0.25 mol kg^{-1}; (c,f) 0.35 mol kg^{-1}.

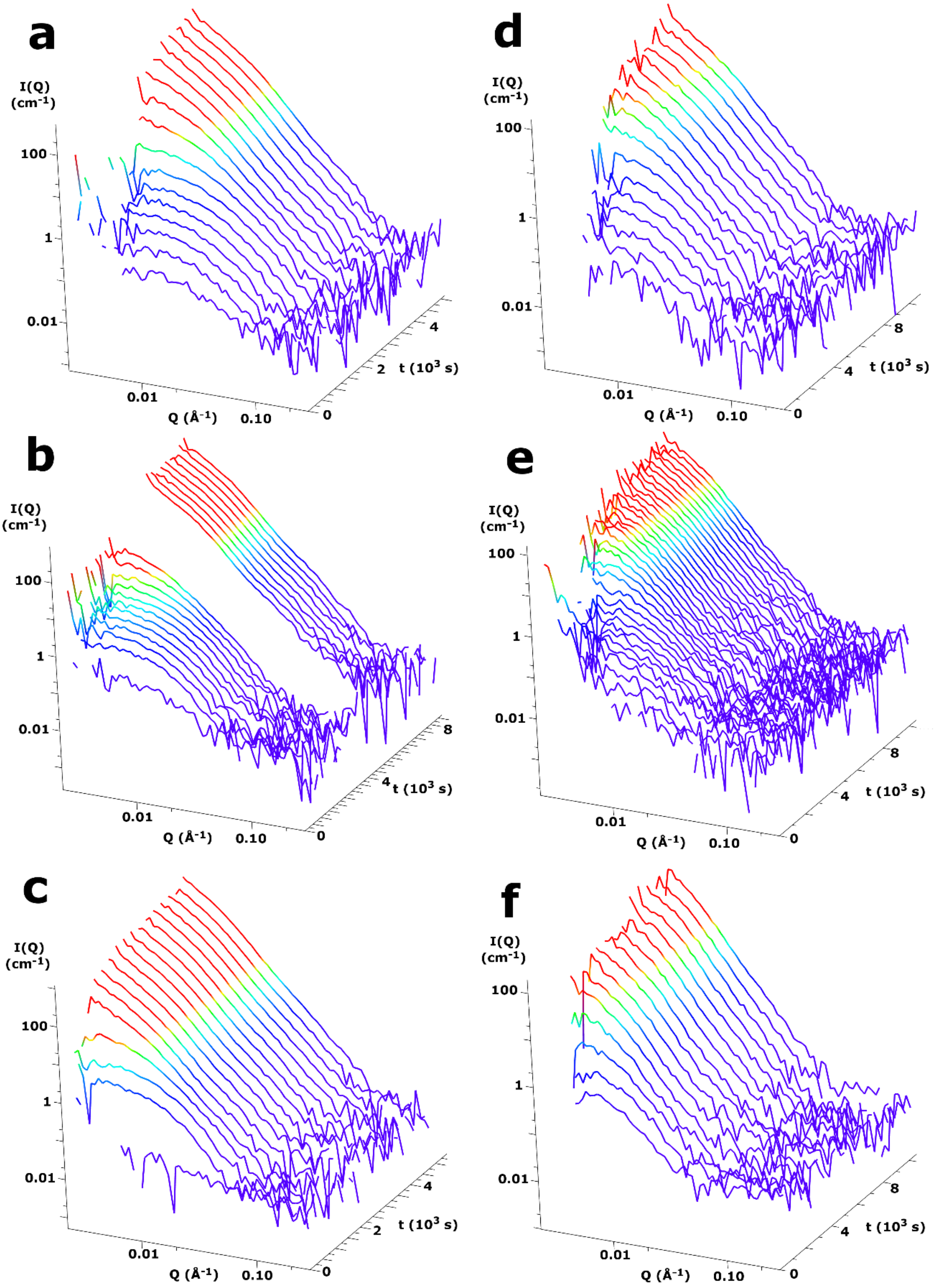

Figure S5. Time-resolved SANS data taken on the BILBY instrument at ANSTO for the hydrated (10*w*) DES as a function of initial $Fe(NO_3)_3.9H_2O$ mole fraction; (a-c) choline chloride:urea:water isotopic composition of H:D:D; (d-f) choline chloride:urea:water isotopic composition of D:D:D; (a,d) 0.15 mol kg^{-1}, (b,e) 0.25 mol kg^{-1}; (c,f) 0.35 mol kg^{-1}. While the water used to formulate the solvent was D_2O, the water of crystallization in the iron nitrate salt was not controlled and will exchange in the mixture to give a non-100% abundance of D_2O. The lost data points in the middle of the medium-concentration, H:D:D sample (b) are due to an instrumental error.

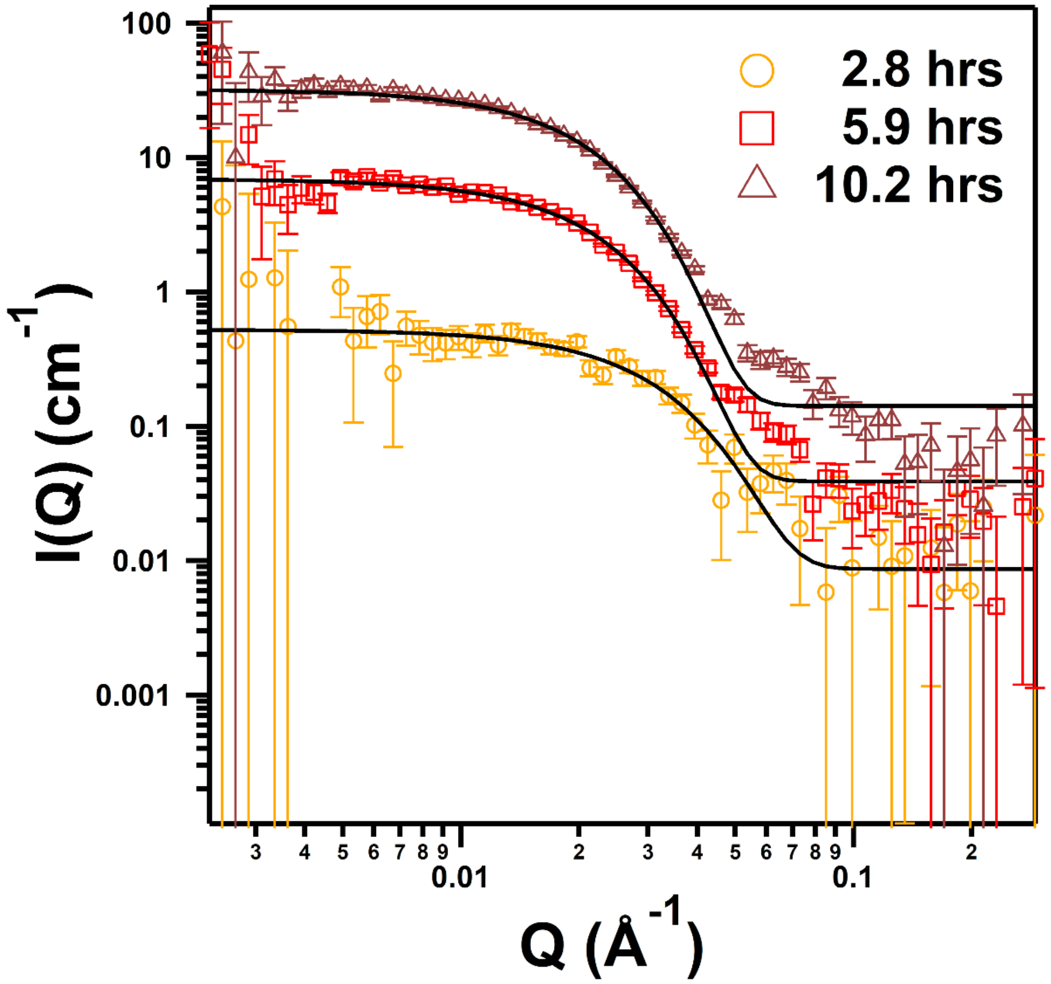

Figure S6. Example SANS data (markers) showing quality of Guinier fits (black lines) for the H:D contrast in the 0.25 mol kg^{-1} of iron nitrate sample. The feature appearing in the 'mid-Q' range (Q = 0.07 Å^{-1}) is most prominent in the H:D contrast shown here. The 'end' sample (t = 10.2 hrs) is offset by y+10 to aid viewing.

Table S2. Computed neutron scattering length densities for the different contrasts, and demonstrating how the solvent SLD changes as a function of water content for 4 different water contents. SLDs are presented here with units of x10^{-6} Å^{-2}. Here, only results for 0*w* (pure solvent) and 10*w* (hydrated solvent, ca. 42 wt.% H_2O) are presented. Calculated values for the 2*w* and 5*w* systems are shown alongside to give an idea of the variation of this parameter as water content is increased.

	0w	**2w**	**5w**	**10w**
D:D:(D)	5.61	5.78	5.96	6.16
H:D:(D)	3.27	3.75	4.26	4.83

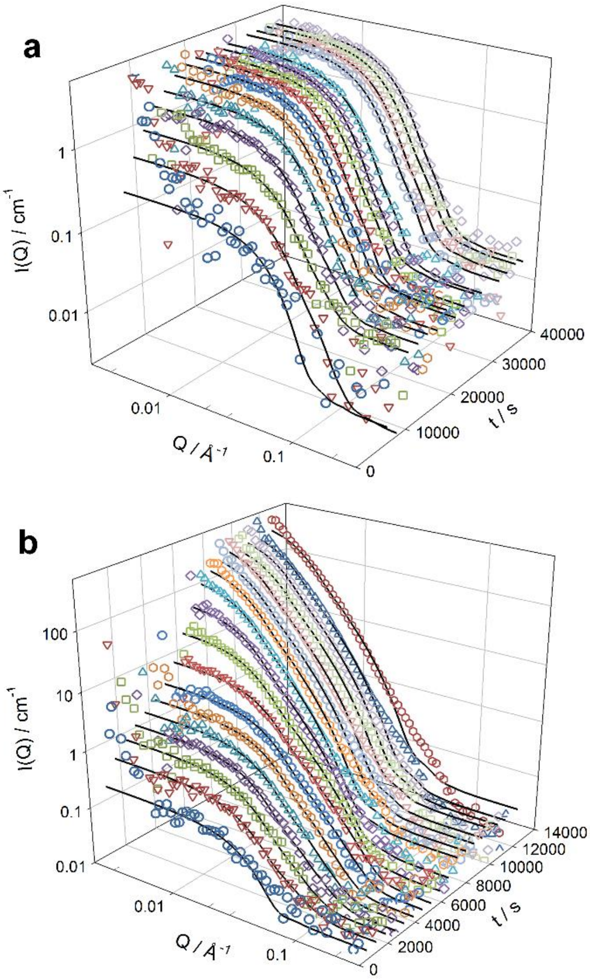

Figure S7. Example data and model-based (oblate-ellipsoid) fits for 0.15 mol kg^{-1} of $Fe(NO_3)_3.9H_2O$ in the pure choline chloride:urea DES in the H:D contrast; (b) example data and model-based (oblate-ellipsoid) fits for 0.15 mol kg^{-1} of $Fe(NO_3)_3.9H_2O$ in the hydrated (10*w*) choline chloride:urea DES in the H:D:D contrast.

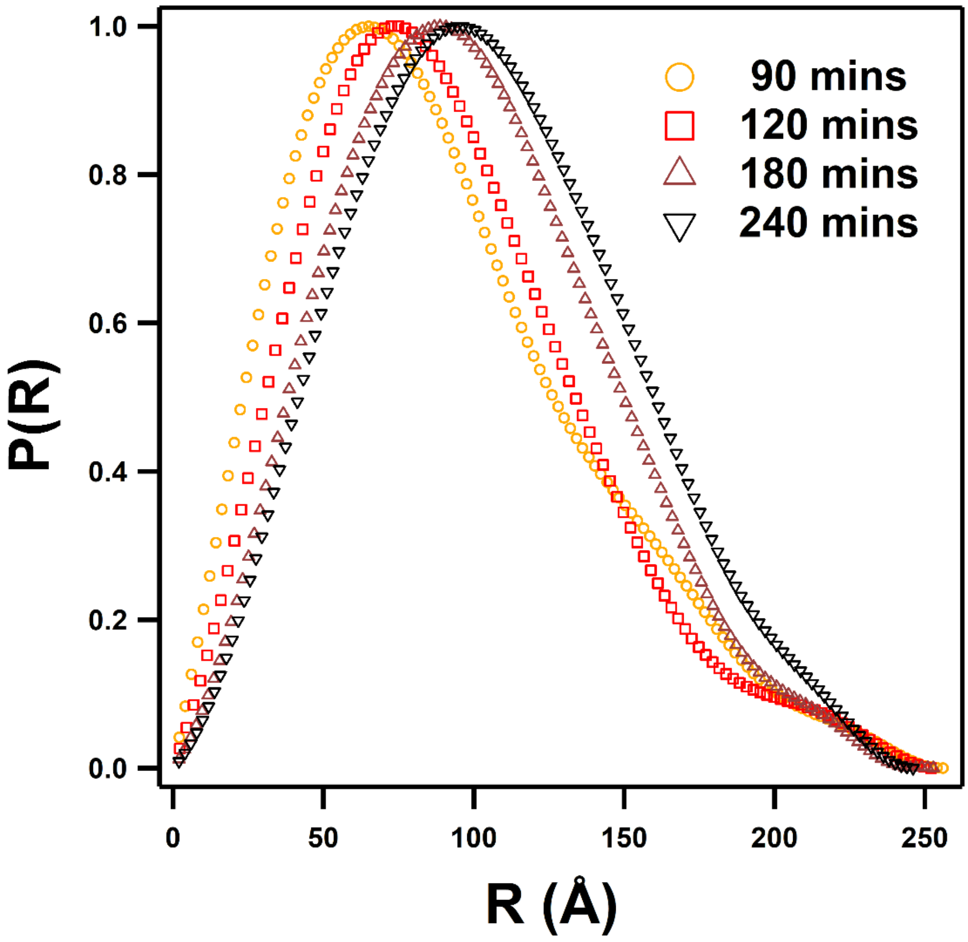

Figure S8. Normalised real-space P(R) inversions of the SAXS data collected for the pure DES systems containing 0.25 mol kg^{-1} of iron precursor, reacted for the listed times in an oven at 90 ˚C.

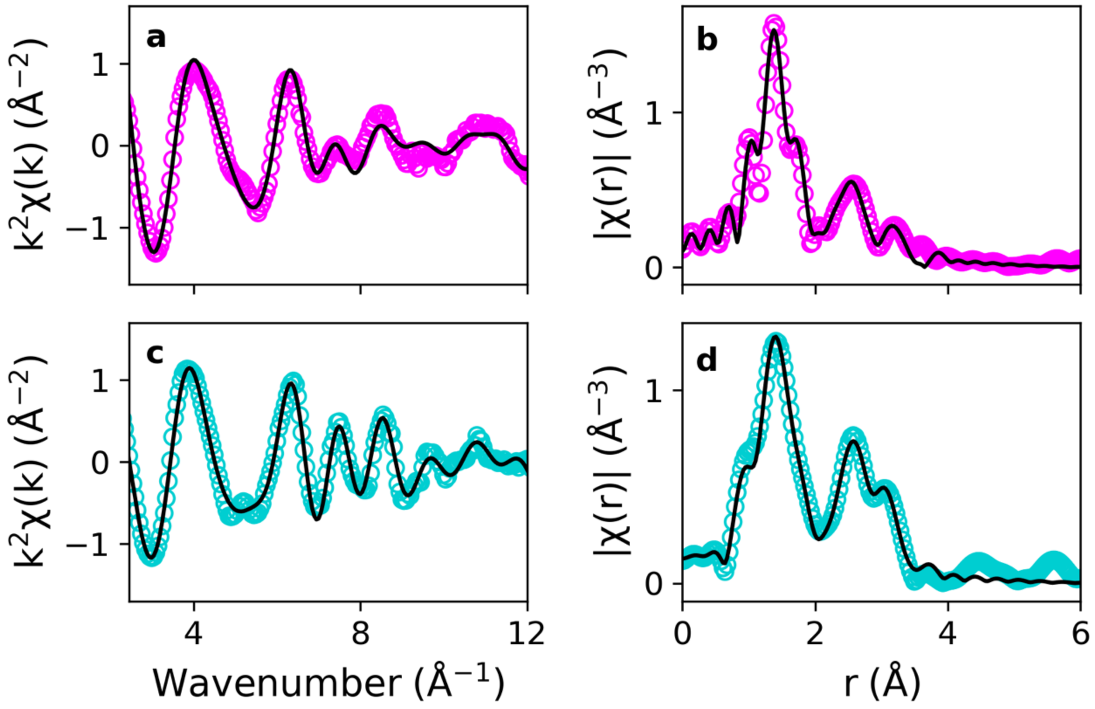

Figure S9. EXAFS data taken of the final state of the pure (magenta) and hydrated (teal) DES systems using I20-Scanning in low-α mode, shown in k-space with k^2 weighting (left; a, c) and r-space (right; b, d). Data are shown as markers, and fits are shown as black lines. Fitting was performed in Artemis, over an r-space range of 1 – 3.47 Å (pure DES) and 1 – 3.53 Å (hydrated DES). Fits were performed by using the hematite crystal structure as a starting point, then optimizing for distances and disorder.

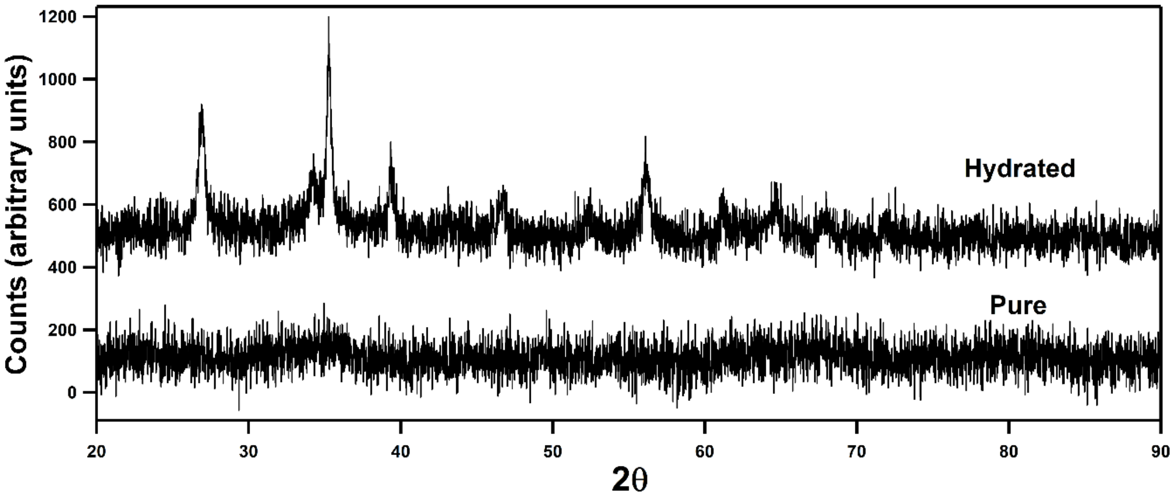

Figure S10. Powder X-Ray diffraction patterns of the isolated products of the off-line solvothermal reactions performed in stainless steel, PTFE-lined autoclaves.

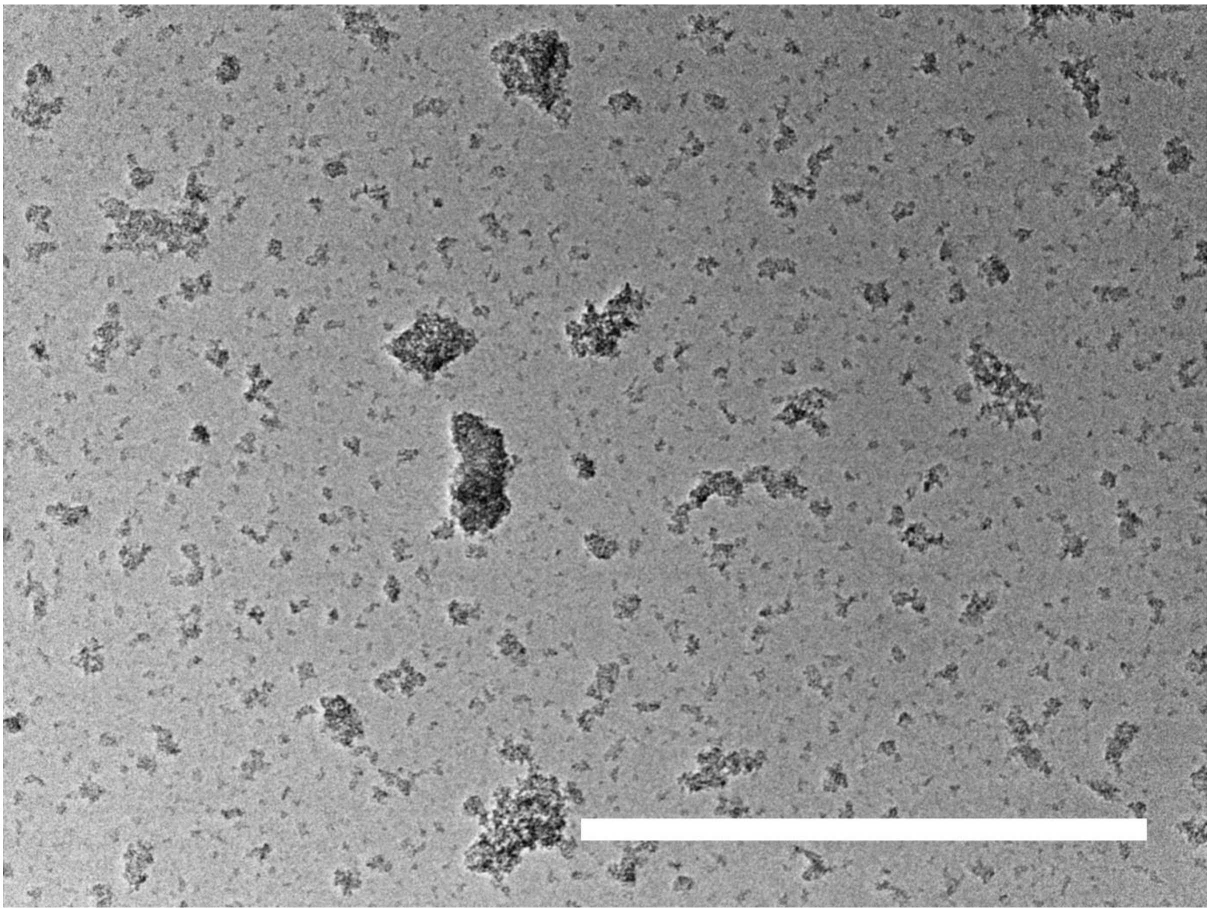

Figure S11. Wide-field transmission electron micrograph of iron oxide NPs and aggregates, from the pure, low-water DES reaction (0.25 mol kg^{-1} of iron nitrate), performed off-line. The scale bar is 500 nm in width.

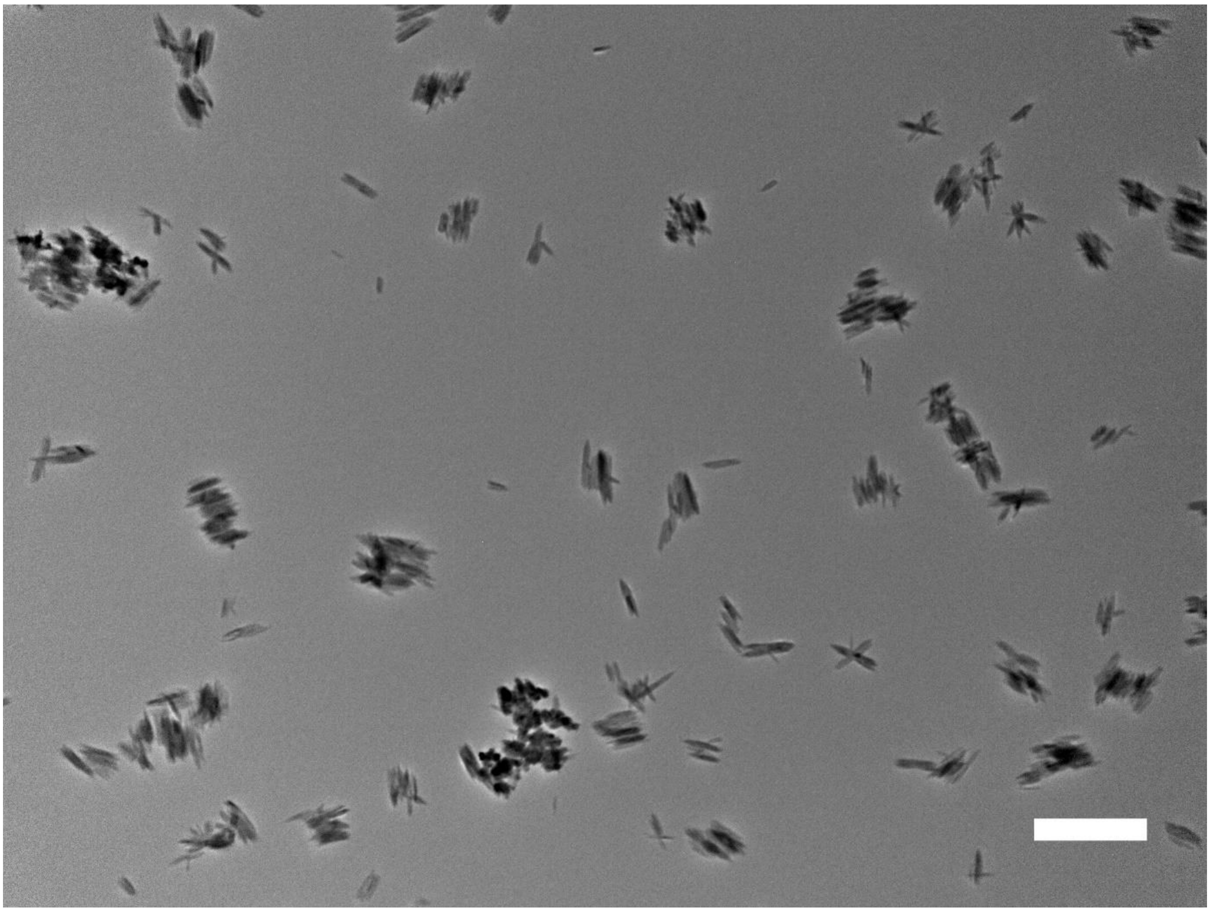

Figure S12. Wide-field transmission electron micrograph of iron oxide NPs and aggregates, from the hydrated, high-water DES reaction (0.25 mol kg^{-1} of iron nitrate), performed off-line. The scale bar is 500 nm in width.

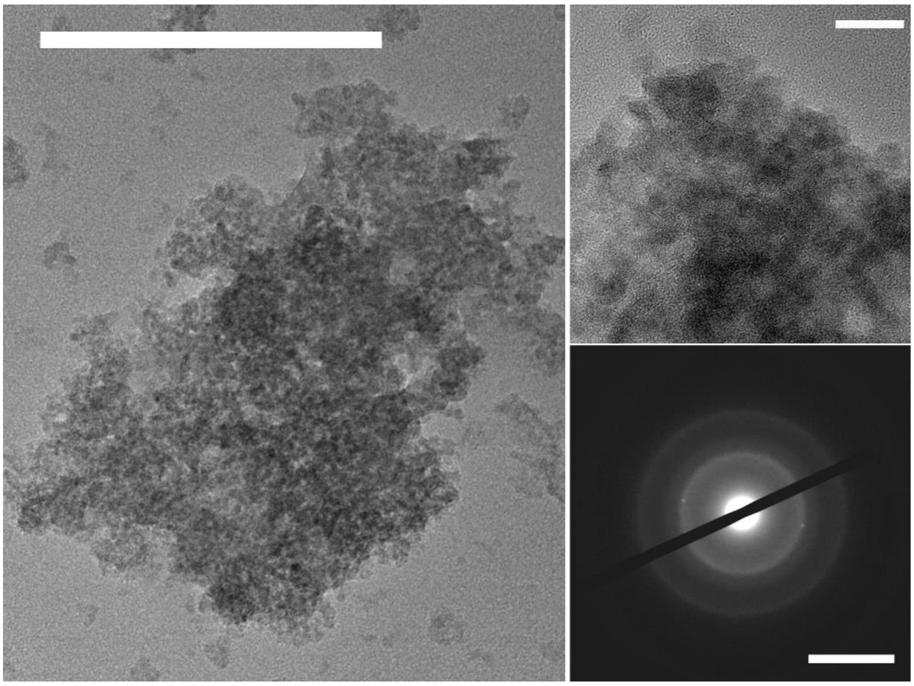

Figure S13. High-magnification transmission electron micrographs of iron oxide NPs from the pure, low-water DES reaction (0.25 mol kg^{-1} of iron nitrate), performed off-line, and (inset, bottom right) electron diffraction (scale = 5 nm^{-1}). Scale bars for the TEM images are 100 nm (left) and 10 nm (top right).

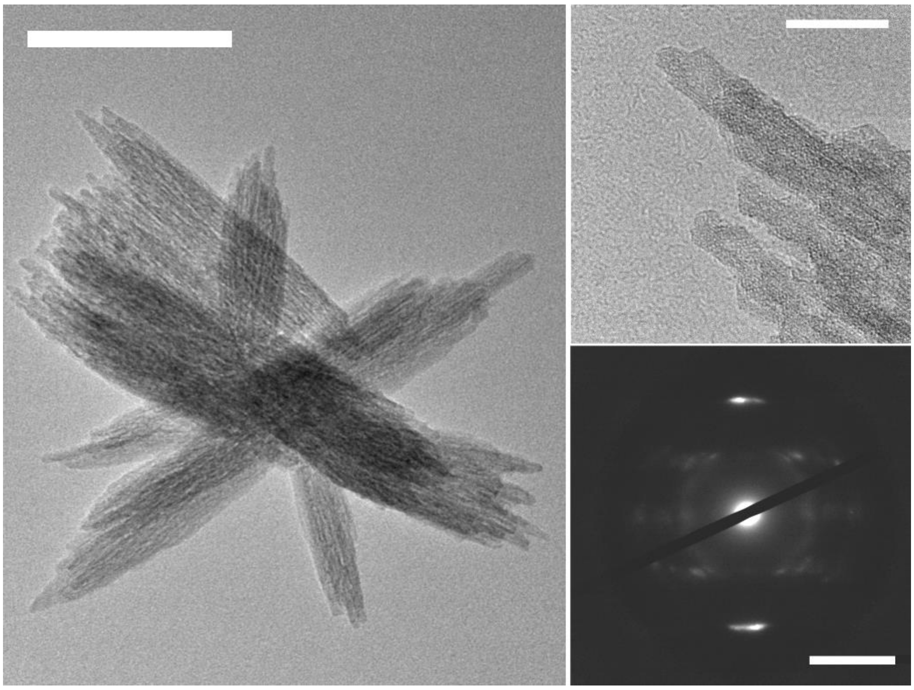

Figure S14. High-magnification transmission electron micrographs of iron oxide NPs produced from the hydrated, high-water DES reaction (0.25 mol kg^{-1} of iron nitrate), performed off-line, and (inset, bottom right) electron diffraction (scale = 5 nm^{-1}). Scale bars for the TEM images are 100 nm (left) and 10 nm (top right).

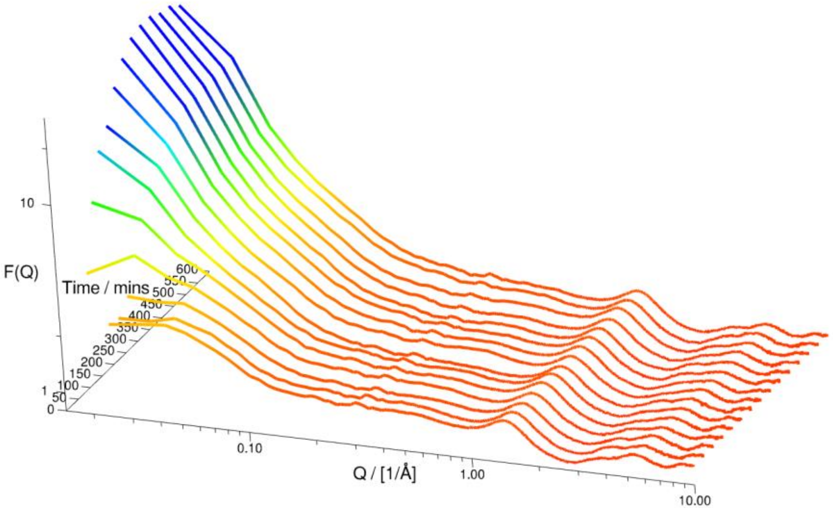

Figure S15. Kinetic measurements of 0.25 mol kg^{-1} of iron nitrate in the pure DES, taken for the fully protonated solvent, in the total scattering instrument NIMROD.

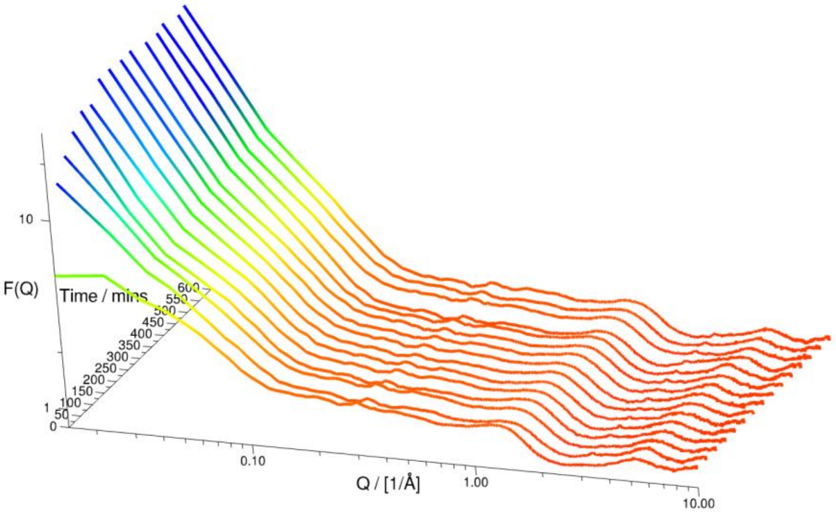

Figure S16. Kinetic measurements of 0.25 mol kg^{-1} of iron nitrate in the hydrated DES, taken for the fully protonated solvent, in the total scattering instrument NIMROD.